ELSEVIER

NeuroImage

www.elsevier.com/locate/ynimg
NeuroImage 26 (2005) 891–899

Frontal circuitry degradation marks healthy adult aging: Evidence from diffusion tensor imaging

Adolf Pfefferbaum,[a,b] Elfar Adalsteinsson,[c,d] and Edith V. Sullivan[b,*]

[a]*Neuroscience Program, SRI International, USA*
[b]*Department of Psychiatry and Behavioral Sciences, Stanford University School of Medicine, 401 Quarry Road, Stanford, CA 94305, USA*
[c]*Department of Electrical Engineering and Computer Science, MIT, Cambridge, MA 02139, USA*
[d]*Harvard-MIT Division of Health Sciences and Technology, MIT, Cambridge, MA 02139, USA*

Received 6 December 2004; revised 14 February 2005; accepted 23 February 2005
Available online 7 April 2005

In vivo study of white matter microstructural integrity through magnetic resonance diffusion tensor imaging (DTI) permits examination of degradation of axonal circuitry that may underlie functional decline of frontally-based processes in normal adult aging. Determination of the pattern of age-related degradation of white matter microstructure requires quantitative comparison of the rostral–caudal and superior–inferior extents of the brain's white matter. To date, this has not been accomplished, probably because of significant artifacts from spatial distortion and poor signal resolution that precludes accurate analysis in prefrontal and inferior brain regions. Here, we report a profile analysis of the integrity of white matter microstructure across the supratentorium and in selected focal regions using DTI data collected at high-field strength (3 T), with isotropic voxel acquisition, and an analysis based on a concurrently-acquired field map to permit accurate quantification of artifact-prone, anterior and inferior brain regions. The groups comprised 10 younger and 10 older individuals; all were high functioning, highly educated, and in excellent health. The DTI profile analysis revealed a robust frontal distribution of low white matter anisotropy and high bulk mean diffusivity in healthy older compared with younger adults. In contrast to frontal fiber systems, posterior systems were largely preserved with age. A second analysis, based on focal samples of FA, confirmed that the age-related FA decline was restricted to frontal regions, leaving posterior and inferior brain regions relatively intact. The selective decline of anterior anisotropy with advancing age provides evidence for the potential of a microstructural white matter mechanism for the commonly observed decline in frontally-based functions.

Keywords: Diffusion; Tensor; White matter; Normal aging

Introduction

The constellation of frontal lobe processes called executive functions–problem solving, working memory, and dual tasking–is especially vulnerable to undesirable effects of advancing age. Although controversy exists regarding the frontal lobe aging hypothesis (Greenwood, 2000), substantial evidence supports the position that aging disproportionately affects frontal lobe structure (e.g., Decarli et al., 2005; Pfefferbaum et al., 1998; Raz et al., 1997). Identification of brain mechanisms responsible for this time-linked demise of multi-dimensional cognitive functions has shifted from exclusive focus on brain gray matter loci to include white matter systems necessary to form neural circuits encompassing frontal processing sites (cf., Filley, 2001; Greenwood, 2000; Tisserand and Jolles, 2003). This shift in focus arises from several lines of evidence and logic. Firstly, the execution of executive functions becomes inefficient but not impossible with advancing age. This pattern of compromise is to be distinguished from that observed in patients with focal cortical lesions, which can result in complete loss of function. Secondly, although quantitative longitudinal neuroimaging studies report accelerated volume loss in prefrontal gray matter with age (Pfefferbaum et al., 1998; Raz, 2004), MR spectroscopic imaging work indicates that signs of neural integrity, for example, the concentration of N-acetylaspartate (NAA), does not decline with age when the volume of underlying cortical gray matter is taken into account (Pfefferbaum et al., 1999b); the normal pattern is different from that in degenerative conditions, such as Alzheimer's disease, which does show decline in the concentration of NAA in gray matter (Adalsteinsson et al., 2000; Pfefferbaum et al., 1999a). Thirdly, neuropathological studies of white matter indicate that frontal white matter systems develop later in youth and deteriorate earlier in aging than posterior ones (Bartzokis, 2004; Marner et al., 2003). Finally, functional imaging studies of normal aging provide converging evidence for the recruitment by older individuals of wider-spread brain systems especially when performing frontally-based tasks to achieve performance levels of younger adults

* Corresponding author. Fax: +1 650 859 2743.
E-mail address: edie@stanford.edu (E.V. Sullivan).
Available online on ScienceDirect (www.sciencedirect.com).

1053-8119/$ - see front matter © 2005 Elsevier Inc. All rights reserved.
doi:10.1016/j.neuroimage.2005.02.034

(Cabeza et al., 2002). An implication of these studies is that in vivo attempts to identify structural substrates of age-related frontal compromise in the normal healthy brain require methods that examine micro-environment of white matter circuitry, in addition to bulk volume differences, which is within the scope of DTI quantification. Further, to make claims about the selective vulnerability of frontal brain regions to aging, frontal sites must be examined within the context the rest of the brain.

MR diffusion tensor imaging (DTI) is a non-invasive, in vivo method for characterizing the integrity of the microstructure of white matter fibers (for reviews, Kubicki et al., 2002; Le Bihan, 2003; Moseley, 2003; Pfefferbaum and Sullivan, 2005a; Sullivan and Pfefferbaum, 2003) and cortical connectivity (e.g., Bammer et al., 2003; Mori et al., 2002; Virta et al., 1999). DTI takes advantage of the linear structure of axons (Greek for axis). Extracellular spaces between fibers harbor fluid and provide avenues for water movement in white matter. Physical trauma, disease, and aging can perturb the axonal linear orientation (Arfanakis et al., 2002), availing white matter constituents and interstitial space to quantitative examination with DTI through quantification of Brownian motion of water molecules within an imaged voxel. Although DTI may not be sensitive enough to directly assess microtubule structure (Beaulieu and Allen, 1994), it can provide information about axonal membrane and myelin presence and integrity (Fenrich et al., 2001; Sehy et al., 2002). The path of a water molecule in a white matter fiber is typically anisotropic because it is constrained by physical boundaries, causing the movement to be greater along the long axis of the fiber than across it. With DTI, tissue can be characterized in terms of the magnitude and orientation of water diffusion, expressed as fractional anisotropy (FA), the fraction of the motion within a voxel that is constrained by physical boundaries (Basser and Pierpaoli, 1996).

Following the early developmental years, the normal adult brain continues to undergo considerable morphological change as it ages. Postmortem investigations reveal degradation of white matter microstructure (Kemper, 1994) and include evidence for decline in numbers of myelinated fibers of the precentral gyrus and corpus callosum. Small connecting fibers of the anterior corpus callosum are especially vulnerable in aging, and their disruption may contribute to age-related declines in cognitive processes dependent on functioning of the prefrontal cortical circuitry (Craik et al., 1990; Raz, 2004). Degradation of myelin and even axon deletion also accompanies normal aging (Aboitiz et al., 1996; Meier-Ruge et al., 1992). These defects in white matter microstructure are beyond detection with conventional structural MRI but are within the scope of DTI quantification.

To date, DTI studies of normal aging have identified declines in anisotropy in a variety of focal white matter regions in normal healthy men and women (Chun et al., 2000; Head et al., 2004; Nusbaum et al., 2001; O'Sullivan et al., 2001; Pfefferbaum and Sullivan, 2003; Pfefferbaum et al., 2000a; Sullivan et al., 2001; but see Chepuri et al., 2002), even when volume declines were not detectable [for review (Sullivan and Pfefferbaum, 2003)]. These focal studies have revealed substantial regional variability (~43%) in FA across the seven decades of the normal adult age range (Pfefferbaum and Sullivan, 2003); some studies identify greater age differences in frontal than posterior white matter (Head et al., 2004). Nonetheless, demonstration of a complete anterior–posterior gradient in age-related FA changes requires quantitative comparison of both the anterior–posterior and superior–inferior extents of the brain's white matter, which has not yet been accomplished, probably because of significant artifacts from spatial distortion and poor signal resolution that precludes accurate analysis in prefrontal and inferior brain regions.

Here, we report a anterior–posterior profile analysis of the integrity of white matter microstructure across the supratentorium and in selected focal regions using DTI data collected at high field strength (3 T), with isotropic voxel acquisition, and an analysis to permit accurate quantification of artifact-prone, anterior and inferior brain regions. Early DTI studies used thick slices with high in-plane resolution, allowing for adequate SNR and visually appealing images. The signal-to-noise advantage at 3 T over 1.5 T permitted collection of thin slices and isotropic data. Thus, we designed a DTI-structural acquisition procedure at 3 T for which we applied correction of B_0 inhomogeneity distortion with improved image segmentation and spatial registration for whole brain and focal region analysis techniques. The profile analysis provided a supratentorial survey of the anterior to posterior and lateral extents of the brain that permitted visual identification and quantitative analysis of regions showing the greatest age differences. The follow-up focal analysis examined samples of maximally-volumed FA in the regions of high or low FA identified with the profile analysis plus other selected regions and permitted direct statistical testing of group-by-region interactions.

Methods

Subjects

Two groups of healthy, highly educated adults were studied: 10 younger (mean = 28.6, range = 22–37 years, 17.2 years of education; 5 men, 5 women) and 10 older (mean = 72.2, range = 65–79 years, 16.3 years of education; 5 men, 5 women). The younger subjects included laboratory members and men and women recruited from the local community. All older subjects were recruited from a larger ongoing study of normal aging and scored well within the normal range on dementia screening tests: Mini-Mental State Examination (Folstein et al., 1975) mean = 28.9, range = 27–30 out of 30 and the Dementia Rating Scale (Mattis, 1988) mean = 140.1, range = 138–143 out of 144.

MRI and DTI acquisition protocol

The DTI-structural acquisition and analysis incorporated correction of spatial distortion due to main field (B_0) inhomogeneity. MRI data were acquired on a 3-T General Electric (Milwaukee, WI) Signa human MRI scanner (gradient strength = 40 mT/m; slew rate = 150 T/m/s; software version VH3). The following four sequences were collected:

(a) Structural fast spin echo (FSE; FOV = 24 cm, TR = 10,000 ms TE = 14/98 ms, thick = 2.5 mm, skip = 0, slice locations = 62);
(b) Inversion Recovery Prepared SPoiled Gradient Recalled echo (IRPrepSPGR; FOV = 24 cm, TI = 300 ms, TR/TE = 6.5/1.54 ms, thick = 1.25 mm, slices = 124);
(c) Diffusion Tensor Images (DTI; FOV = 24 cm, TR = 11,000 ms TE = 97.6 ms, thick = 2.5 mm, skip = 0, slice locations = 62, 0 (8 NEX) + 6 non-collinear diffusion directions (4 NEX, gradient orientations $+x +y$, $+y +z$, $+x +z$, $-x +y$, $-y$

$+z$, $+x$ $-z$ with a repeat of these six orientations with opposite gradient polarity, 1.45 Gauss/cm with 32 ms duration and 38 ms separation, resulting in a b value of 860 s/mm^2, x-dim = 96, y-dim = 96, 3472 total images);

(d) Fieldmap (FOV = 24 cm, multislice, dual echo, single-shot spiral acquisition, x-dim = 128, y-dim = 128).

The SPGR data were aligned such that two 1.25-mm slices subtended each 2.5 mm thick FSE and DTI slice with custom scanner prescription software, which computed precise slice locations. The data from the spiral acquisition for each echo were gridded and Fourier transformed, and a fieldmap was estimated from a complex difference image between the two echoes (Pfeuffer et al., 2002).

DTI analysis

DTI quantification was preceded by eddy current correction using a template made from an average image created across all gradient directions and a 2-D, 6-parameter affine warp on a slice-by-slice basis (Woods et al., 1998). Using the field maps, B_0-field inhomogeneity-induced geometric distortion in the eddy current-corrected images was corrected with FUGUE (FMRIB's Utility for Geometrically Unwarping EPIs) (Jenkinson, 2003). Next, the $b = 0$ images were warped to the late echo FSE images in 3-D, first with a 12-parameter affine, followed by stepwise 2nd and 3rd order polynomial functions. This transformation was then applied to all B_0 field-corrected and eddy current-corrected averaged images (Fig. 1). Finally, using the corrected images, $b = 0$ and $b = 860$ s/mm^2, 6 maps of the apparent diffusion coefficient (ADC) were calculated. Solving 6 simultaneous equations with respect to ADCxx, ADCxy, etc. yielded the elements of the diffusion tensor. The diffusion tensor was then diagonalized, yielding eigenvalues λ_1, λ_2, λ_3, as well as eigenvectors that define the predominant diffusion orientation. Based on the eigenvalues, the fractional anisotropy (FA) and bulk mean diffusivity (the mean of the eigenvalues, $<D>$) were calculated on a voxel-by-voxel basis (Basser and Jones, 2002; Basser and Pierpaoli, 1998; Pierpaoli and Basser, 1996).

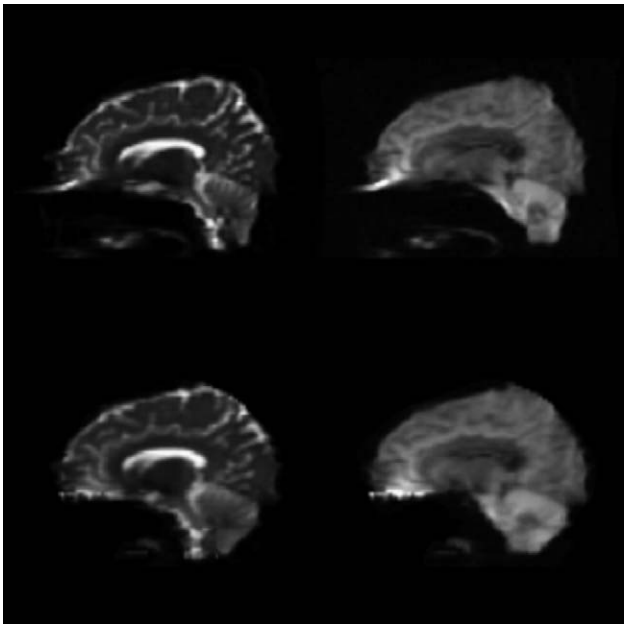

Fig. 1. Reconstructed mid-sagittal echo-planar (left) and diffusion weighted (right) images before (top) and after (bottom) B_0 field inhomogeneity correction. The correction is based on a measured field map and the timing parameters of the echo-planar readout applied in the DTI acquisition.

Segmentation

The brain was extracted from the intracranial cavity with FSL Brain Extraction Tool (BET) (Smith, 2002) applied to the early echo FSE images and segmented into three compartments (gray matter, white matter, and CSF) with FSL mFAST (Smith, 2002; Zhang et al., 2001) applied to three channels (SPGR, early and late echo FSE).

Warping to common coordinates

To place the images for all subjects into a coordinate system with a common origin and a standardized anatomical orientation, the anterior commissure (AC) and posterior commissure (PC) were manually identified on the native 1.25 mm-thick SPGR images. The AC was shifted to a fixed coordinate in the anterior/posterior orientation, and the image volume was oriented by three rotations with the AC as the pivot point. After this shift and rotations, the original oblique-axial plane that passed through the AC and PC was a straight axial section perpendicular to the midsagittal plane. The parameters required to accomplish this transformation for each scan session were applied to all of the structural images and the FA and segmented images. Finally, all of the datasets were resliced to isotropic 1 mm^3 voxels and the field-of-view set to 20 cm for each axis. This image volume was large enough to encompass the entire brain for all subjects in the study.

Profile analysis

First, a grand average SPGR data set was created from all 20 subjects. This average was then used as a template upon which each subject was aligned (individual SPGR to template SPGR) with a 12-parameter affine model, followed by creation of a new grand average used as a template for a higher-order (3rd to 5th polynomial) nonlinear warp. The alignment parameters were then applied to the FA and segmentation data for each subject, and new grand averages by group were constructed for display purpose. The use of nonlinear warping allowed the registration of young and old brains to a common space despite age-related differences in morphology, for instance, of the corpus callosum that expands in height and length with age (Pfefferbaum et al., 2000b). The same process was used to create the diffusivity profile.

For each subject's group-aligned segmentation images, the white matter skeleton from the segmentation procedure was identified and a 1-mm erosion morphological operator applied across coronal slices to reduce the contribution of partial voluming to the white matter compartment, and a final nonlinear warp of the white matter skeleton to the FA was applied. Each individual's FA data were then masked with his or her white matter compartment to yield the final anisotropy data set.

Focal DTI analysis

One operator (E.V.S.) placed all 18 region-of-interest loci (genu and splenium and bilateral measures of anterior cingulate bundle,

middle frontal gyrus, frontal forceps, posterior forceps, superior longitudinal fasciculus, inferior longitudinal fasciculus, cerebral peduncle, and pontocerebellar tract) in a two-step process. Firstly, each point was placed on grand average data including all 20 subjects. Secondly, these locations were then presented on the FA images for each individual subject for minor spatial location adjustment. The placement decision was aided by having a simultaneous display, with cross-hairs, of images in the three orthogonal planes (sagittal, coronal, and axial) and the interactive capability of moving the point placement in the three planes simultaneously. This interactive mode facilitated implementation of predetermined rules for anatomical location identification. Each adjusted point was then dilated to produce a 5-mm^3 volume, which determined the region of interest from which FA and <*D*> were measured. Manual location of regions was performed blind to all subject identification, and warping each subject to a common size obscured differences in appearance related to sex and age.

Results

Profile analysis

Slice-by-slice profiles (Fig. 2) of the mean FA in segmented white matter visually depicts the distribution of values across the anterior-to-posterior extents of the supratentorium (defined as all white matter superior to the AC–PC plane) for each age group. Profiles from three regions are presented: left hemisphere, right hemisphere, and a 10-mm section at the midline. The statistical results of two group comparisons for each coronal slice are presented above the *x* axis for each profile. The *t* test comparisons indicated that the most striking and highly significant group differences were in the frontal areas and always favored the younger group, whereas the central and posterior white matter FA showed no age effect.

Frequency counts of the number of slices showing significantly lower FA in older than younger subjects were determined for the three profiles. Each was based on slices 24 to 171, which had FA values greater than 0. The proportions of slices yielding significant group differences were 74% for the left hemisphere, 71% for the right hemisphere, and 46% for the midline region. For the total supratentorial FA measure, 115 of the 147 slices (78%) with FA values greater than 0 showing significant group differences were divided into anterior and posterior regions at slice 100. The anterior 76 of 77 slices (99%) had *P* values at 0.02 or below, whereas only the posterior 39 of 72 slices (54%) had *P* values of 0.05 or below.

Profiles of bulk mean diffusivity of the midline and lateral regions complemented the FA profiles. In all three profiles, the anterior but not the posterior regions had significantly higher <*D*> in the older than younger group (Fig. 3).

Focal analysis

As was evident in the profile analysis, age-related differences in focal FA varied significantly across regions but not hemispheres (Fig. 4). Therefore, group differences for each focal region were

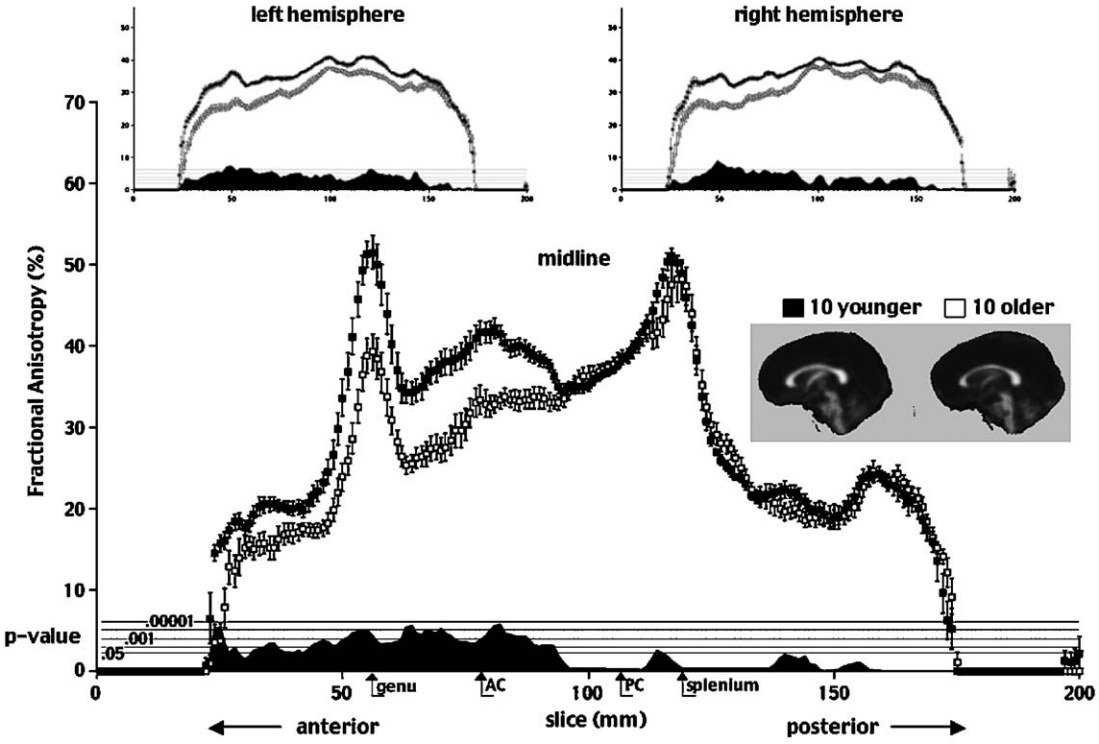

Fig. 2. Profile of mean ± SEM FA in segmentation-defined supratentorial white matter presented slice-by-slice from frontal to occipital brain regions in the 10 young and 10 older healthy subjects. The sagittal brain images are grand averages of FA of the 10 younger and 10 older adults; the corpus callosum is prominent in cross-section. The large profile is taken from the medial 10 mm of the brain; the small profiles are taken from white matter lateral to the midline values. Note the systematic FA difference in the anterior regions with higher FA in the younger compared with older subjects. The black mounds on the *x* axis indicate the *P* value for group differences for each slice. The gray horizontal lines over the mounds designate *P* values, with the bottom line being $P = 0.05$ and the top line $P = 0.00001$.

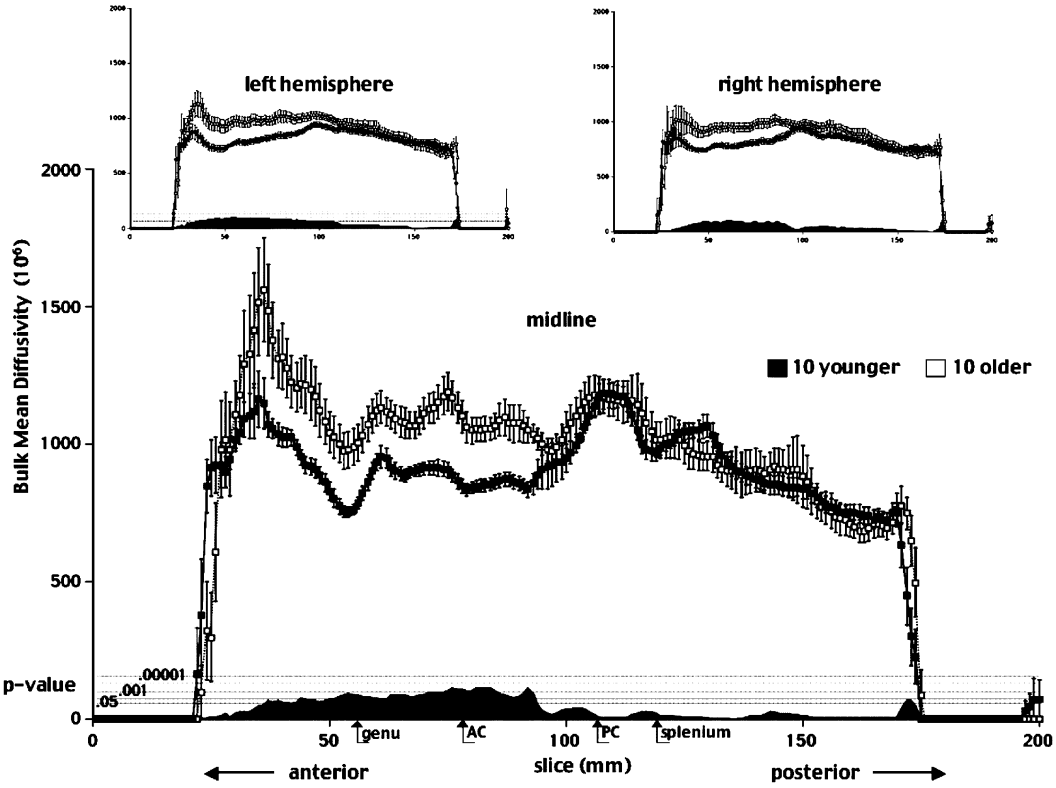

Fig. 3. Profile of mean ± SEM bulk mean diffusivity (<*D*>) in segmentation-defined supratentorial white matter presented slice-by-slice from frontal to occipital brain regions in the 10 young and 10 older healthy subjects. The large profile is taken from the medial 10 mm of the brain; the small profiles are taken from white matter lateral to the midline values. Note the systematic <*D*> difference in the anterior regions, with higher <*D*> in the older relative to the younger subjects. The black mounds on the *x* axis indicate the *P* value for group differences for each slice. The gray horizontal lines over the mounds designate *P* values, with the bottom line being $P = 0.05$ and the top line $P = 0.00001$.

based on the mean FA of the left and right hemispheres for a given region. The older group had lower FA than the younger group in the superior ($t(18) = 4.166$, $P = 0.0006$) and inferior ($t(18) = 4.155$, $P = 0.0006$) longitudinal fasciculi, anterior cingulate bundle ($t(18) = 3.390$, $P = 0.0033$), middle frontal gyrus ($t(18) = 3.304$, $P = 0.0039$), frontal forceps ($t(18) = 7.078$, $P = 0.0001$), and genu ($t(18) = 4.122$, $P = 0.0006$). In contrast to these anterior foci, the groups did not differ in mean FA in posterior regional foci: posterior forceps ($t(18) = 0.076$, $P = 0.94$), cerebral peduncle ($t(18) = 1.226$, $P = 0.236$), pontocerebellar tract ($t(18) = 0.024$, $P = 0.98$), and splenium ($t(18) = 0.070$, $P = 0.95$).

To challenge whether the anterior distribution of the profile analysis was present in FA of focal fiber tracts, group-by-region analysis of variance tested the anterior vs. posterior FA in two pairs of regions: frontal vs. posterior forceps and genu vs. splenium. In both cases, the interaction was significant (forceps $F(1,18) = 30.967$, $P = 0.0001$; corpus callosum $F(1,18) = 20.771$, $P = 0.0002$), indicating that the frontal region was disproportionately affected relative to the posterior region in the older group.

Group differences were also examined in regional <*D*>. As with FA, <*D*> varied across regions but not hemispheres (Fig. 5). Thus, group comparisons were based on the mean <*D*> of the left and right hemispheres for each region. The older group had higher <*D*> than the younger group in the superior ($t(18) = 3.285$, $P = 0.0041$) and inferior ($t(18) = 2.562$, $P = 0.0196$) longitudinal fasciculi, anterior cingulate bundle ($t(18) = 4.328$, $P = 0.0004$), middle frontal gyrus ($t(18) = 3.134$, $P = 0.0057$), frontal forceps ($t(18) = 2.381$, $P = 0.0285$), and genu ($t(18) = 2.907$, $P = 0.0094$). In contrast to these anterior foci, the groups did not differ significantly in mean <*D*> in posterior regional foci: posterior forceps ($t(18) = 1.370$, $P = 0.188$), cerebral peduncle ($t(18) = 1.363$, $P = 0.190$), pontocerebellar tract ($t(18) = 1.419$, $P = 0.173$), and splenium ($t(18) = 0.042$, $P = 0.97$). Repeated measures group-by-region ANOVAs examining frontal versus posterior regional <*D*> yielded a significant interaction for the genu-splenium comparison ($F(1,18) = 10.666$, $P = 0.0043$) and a trend for the frontal–posterior forceps comparison ($F(1,18) = 3.130$, $P = 0.0938$).

In a final set of analyses, we first examined the relationships between regional diffusivity and anisotropy in the frontal regions where age effects were prominent. In the older group, <*D*> showed significant negative correlations with FA in the frontal forceps ($r = -0.74$, $P = 0.0139$), anterior cingulum ($r = -0.78$, $P = 0.0084$), and genu ($r = -0.94$, $P = 0.0001$) but not the medial frontal gyrus ($r = -0.42$, $P = 0.2239$). These correlations were not significant in the younger group (frontal forceps $r = 0.39$; anterior cingulum $r = -0.26$; genu $r = -0.21$; and medial frontal gyrus $r = -0.27$). We then used multiple regression in the younger and older groups combined to test whether age and the magnitude of diffusivity each made unique contributions to the variance of FA in three frontal regions with significant <*D*> with FA correlations. <*D*> made a significant and unique contribution, over and above age, to FA in all three regions: frontal forceps (partial $F = 60.05$, $P = 0.0001$), anterior cingulum (partial $F = 11.31$, $P = 0.0037$), and genu (partial $F = 52.92$, $P = 0.0001$). By contrast, age's contribution to FA after accounting for the contribution from <*D*> was significant for the frontal forceps (partial $F = 7.67$ $P = 0.0131$) and the genu

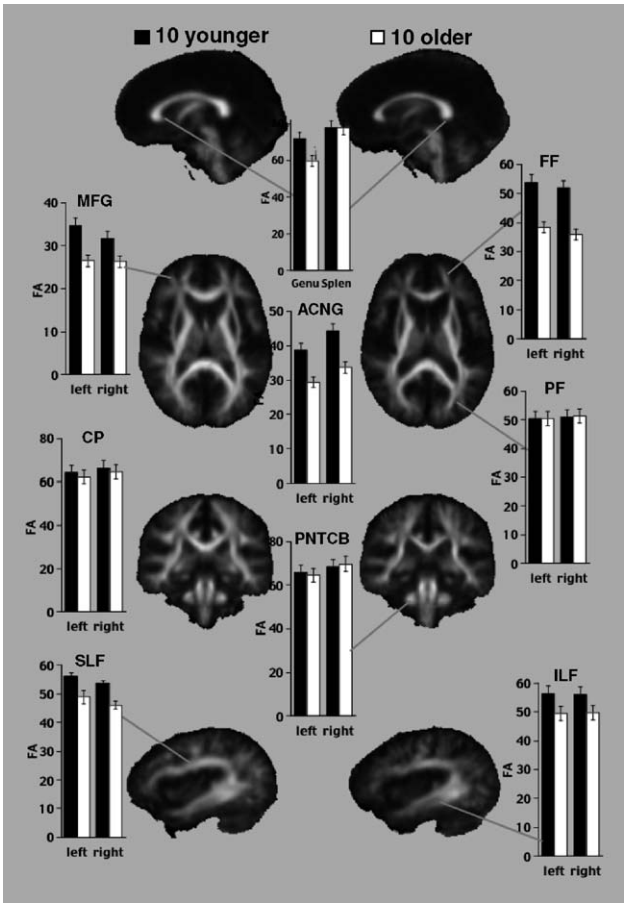

Fig. 4. Mean ± SEM for focal regional FA for the younger and older groups. The FA images are grand averages of the 10 younger and 10 older healthy subjects warped to a common template. SLF, superior longitudinal fasciculus; ILF, inferior longitudinal fasciculus; FF, frontal forceps; PF, posterior forceps; MFG, middle frontal gyrus; ACNG, anterior cingulate bundle; CP, cerebral peduncle; PNTCB, pontocerebellar tract; Genu; and Splen = splenium.

(partial $F = 6.98$, $P = 0.0171$) but not the anterior cingulum (partial $F = 0.04$, $P = 0.84$). To test whether the age versus diffusivity effect was selective to anterior regions, we next performed these multiple regression analyses for the posterior forceps and the splenium. For both regions, <*D*> was a significant and unique predictor of FA (posterior forceps partial $F = 8.52$, $P = 0.0096$; splenium partial $F = 23.83$, $P = 0.0001$) but age was not (posterior forceps partial $F = 0.92$, $P = 0.35$; splenium partial $F = 0.01$, $P = 0.91$).

Discussion

This DTI analysis revealed a robust frontal distribution of low white matter anisotropy and high diffusivity in healthy older compared with younger adults. In contrast to frontal fiber systems, posterior systems were largely preserved with age. This pattern of greater anterior than posterior age-related declines in white matter anisotropy was present whether analyzed with the profile or the focal regional approach and may contribute to the explanation of the selective demise of frontally-based functions with advancing age. Image data collection of isotropic voxels at 3 T together with application of a field map permitting correction for B_0 field inhomogeneity yielded a basis for error-reduced quantification of FA in the frontal and inferior regions, which especially suffer inhomogeneity artifact and reduce accuracy in attempts to quantify anisotropy (Bammer et al., 2003; Jones et al., 2002; Le Bihan, 2003; Virta et al., 1999). With these isotropic data, images could be reformatted and resliced in any plane, minimizing partial voluming error or bias that might occur if the through-plane dimension was much smaller than in-plane voxel size (cf., Jones et al., 2002).

Features of normal aging are degradation of myelin and microtubules (Aboitiz et al., 1996; Meier-Ruge et al., 1992) and decline in the number and length of myelinated fibers (Marner et al., 2003). A predilection of loss occurs for thin fibers, which are in greatest abundance in the frontal lobes and develop and mature later than large-diameter axons (Bartzokis, 2004). Small connecting fibers of the anterior corpus callosum are especially vulnerable in aging. Late myelinating fibers are sheathed in thin layers susceptible to injury. One possible cause of injury is that a single oligodendrocyte can myelinate multiple small axons, whereas large diameter axons typically develop early and are myelinated by oligodendrocytes on a 1:1 basis (Bjartmar et al., 1994).

Selective disruption of frontally-based fibers are likely structural substrates of age-related declines in cognitive processes dependent on functioning of the prefrontal circuitry (Raz, 2004).

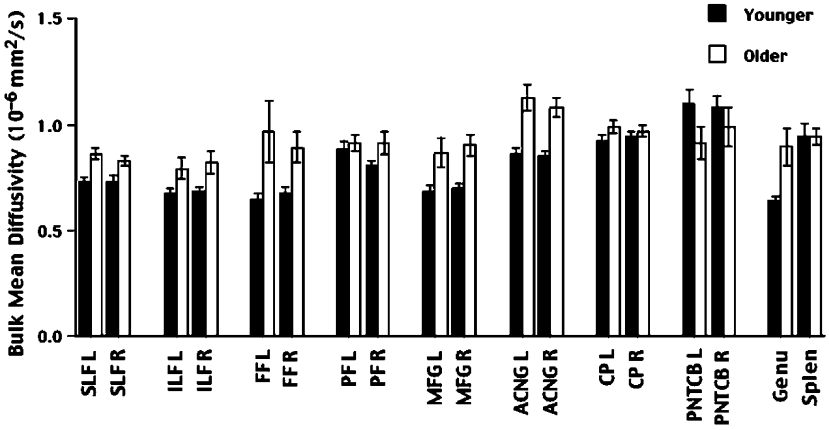

Fig. 5. Mean ± SEM for focal regional bulk mean diffusivity <*D*> for the younger and older groups. SLF, superior longitudinal fasciculus; ILF, inferior longitudinal fasciculus; FF, frontal forceps; PF, posterior forceps; MFG, middle frontal gyrus; ACNG, anterior cingulate bundle; CP, cerebral peduncle; PNTCB, pontocerebellar tract; Genu; and Splen = splenium. For each regional pair, except the genu and splenium, L = left and R = right hemisphere.

Regions exhibiting severe age-related declines in anisotropy include the anterior cingulum and middle frontal gyrus, sites identified in functional imaging studies as comprising the specific frontal network "consistently recruited for solution of diverse cognitive problems," including response selection, executive control, working memory, episodic memory, problem solving, and aspects of perception that require conflict resolution (Duncan and Owen, 2000). As late developers (Sowell et al., 1999), frontal sites are also under proportionately greater environmental than genetic control than posterior regions. Evidence for this differential environmental-genetic control is based on a study, which compared heritability of regional callosal FA in monozygotic (MZ) twin pairs relative to dizygotic (DZ) twin pairs (Pfefferbaum et al., 2001) and revealed that the proportion of genetic to environmental contributions to FA was 3:1 for the splenium but only 1:1 for the genu.

In complement to age-related decline and pattern of FA, bulk mean diffusivity was significantly greater in the older than younger subjects and the locus of the age effect was in anterior white matter. In previous studies, we showed that diffusivity measurements can be inflated by partial voluming; however, even when reduced by eroding peripheral voxels from regions of interest, diffusivity increases with age (Pfefferbaum and Sullivan, 2002, 2003). Further, we observed that low FA was typically associated with high diffusivity. The magnitude of this relationship, however, varied across brain regions, being greater in the centrum semiovale than the corpus callosum, and with age, being greater in older than younger healthy individuals (Pfefferbaum and Sullivan, 2003). In the present study, we again observed the high diffusivity predicted FA both in anterior and posterior regions. This relationship suggests that decreased brain white matter intravoxel coherence is attributable, at least in part, to the accumulation of interstitial or intracellular fluid, or both fluid compartments (e.g., Norris et al., 1994; Pfefferbaum and Sullivan, 2005b; Rumpel et al., 1998; Sehy et al., 2002; Silva et al., 2002). Relevant to the current question regarding the locus of age's effect on anisotropy, we found that age made a unique contribution to low FA selectively to anterior white matter regions. We may speculate from these observations that the age-related lower intravoxel coherence prominent in the frontal regions is indicative of degradation of white matter constituents, such as myelin, which is known from postmortem studies to occur even in normal older nonpathological cases (Aboitiz et al., 1996; Marner et al., 2003).

This study is no exception in having limitations. Among them is the small number of diffusion directions acquired in the DTI sequence. We used six noncollinear directions with opposite gradient polarity. While adequate to calculate the tensor, recent analyses reveal substantially improved data quality with more sampling orientations (Batchelor et al., 2003, 2005; Hasan et al., 2001; Jones, 2004). Using a Monte Carlo simulation, Jones (2004) showed that "at least 20 unique sampling orientations are necessary for a robust estimation of anisotropy, whereas at least 30 unique sampling orientations are required for a robust estimation of tensor-orientation and mean diffusivity" (page 807). Nonetheless, Jones (2004) further noted that the time required to acquire a diffusion sequence with large numbers of orientations is impractical for most human studies and in fact the advantage gained when using more that 10 unique sampling directions is negligible. The procedure described here also involved several sequential resamplings of the data as the analysis evolved; multiple resampling can blur the data, reduce accuracy, and represents a limitation of the current study.

Another limitation concerns cognitive status of the older subjects in this study. Although a large body of studies (for reviews, Buckner, 2004; Hedden and Gabrieli, 2004; Raz, 1999; but see Greenwood, 2000) supports the position that as a group older, healthy individuals are likely to exhibit poorer executive functioning than younger individuals, we do not have neuropsychological test evidence that the subjects of the present study had executive function problems. Indeed, the subjects in the older group were highly educated and had mental status examinations well within the normal range. Thus, it may be especially intriguing that these otherwise intact elders had a profound frontal distribution of low anisotropy and high diffusivity in brain white matter. Future studies designed to replicate the frontal-based pattern of age-related FA decrease and diffusivity increase should also examine different component processes of executive functions that could be disturbed by disruption of focal white matter integrity.

Unlike neurodegenerative diseases and demonstrable neurological events, the effects of normal adult aging are subtle, accrue insidiously, and can be elusive to detection with conventional macrostructural neuroimaging techniques. The present in vivo study of whole brain white matter microstructure revealed that, even if posterior brain systems successfully endure the throes of aging, information flow from them to frontal processing sites could be impeded by a degenerating anterior fiber infrastructure. This possibility can be tested in future studies employing more diffusion directions, larger samples of subjects, and selective behavioral tests to assess the functional ramifications of DTI metrics. Coupling such studies with functional imaging could serve to identify potential age-related differences in the constellation and integrity of white matter networks connecting cortical sites recruited for task performance.

Acknowledgments

This work was supported by NIH grants AG17919, AG18942, AA05965, AA10723, AA12388. We thank Eric Hahn of the Applied Systems Laboratory-West of General Electric Healthcare for providing the prescription software for acquiring fully registered diffusion and structural images.

References

Aboitiz, F., Rodriguez, E., Olivares, R., Zaidel, E., 1996. Age-related changes in fibre composition of the human corpus callosum: sex differences. NeuroReport 7, 1761–1764.

Adalsteinsson, E., Sullivan, E.V., Kleinhans, N., Spielman, D.M., Pfefferbaum, A., 2000. Longitudinal decline of the neuronal marker N-acetyl aspartate in Alzheimer's disease. Lancet 355, 1696–1697.

Arfanakis, K., Haughton, V.M., Carew, J.D., Rogers, B.P., Dempsey, R.J., Meyerand, M.E., 2002. Diffusion tensor MR imaging in diffuse axonal injury. Am. J. Neuroradiol. 23, 794–802.

Bammer, R., Acar, B., Moseley, M.E., 2003. In vivo MR tractography using diffusion imaging. Eur. J. Radiol. 45, 223–234.

Bartzokis, G., 2004. Age-related myelin breakdown: a developmental model of cognitive decline and Alzheimer's disease. Neurobiol. Aging 25, 5–18 (author reply 49–62).

Basser, P.J., Jones, D.K., 2002. Diffusion-tensor MRI: theory, experimental design and data analysis—a technical review. NMR Biomed. 15, 456–467.

Basser, J., Pierpaoli, C., 1996. Microstructural and physiological features of

tissues elucidated by quantitative diffusion tensor MRI. J. Magn. Reson., Ser. B 111, 209–219.
Basser, P.J., Pierpaoli, C., 1998. A simplified method to measure the diffusion tensor from seven MR images. Magn. Reson. Med. 39, 928–934.
Batchelor, P.G., Atkinson, D., Hill, D.L., Calamante, F., Connelly, A., 2003. Anisotropic noise propagation in diffusion tensor MRI sampling schemes. Magn. Reson. Med. 49, 1143–1151.
Batchelor, P.G., Moakher, M., Atkinson, D., Calamante, F., Connelly, A., 2005. A rigorous framework for diffusion tensor calculus. Magn. Reson. Med. 53, 221–225.
Beaulieu, C., Allen, P.S., 1994. Water diffusion in the giant axon of the squid: implications for diffusion-weighted MRI of the nervous system. Magn. Reson. Med. 32, 579–583.
Bjartmar, C., Hildebrand, C., Loinder, K., 1994. Morphological heterogeneity of rat oligodendrocytes: electron microscopic studies on serial sections. Glia 11, 235–244.
Buckner, R.L., 2004. Memory and executive function in aging and AD: multiple factors that cause decline and reserve factors that compensate. Neuron 44, 195–208.
Cabeza, R., Anderson, N.D., Locantore, J.K., McIntosh, A.R., 2002. Aging gracefully: compensatory brain activity in high-performing older adults. NeuroImage 17, 1394–1402.
Chepuri, N.B., Yen, Y.F., Burdette, J.H., Li, H., Moody, D.M., Maldjian, J.A., 2002. Diffusion anisotropy in the corpus callosum. Am. J. Neuroradiol. 23, 803–808.
Chun, T., Filippi, C.G., Zimmerman, R.D., Ulug, A.M., 2000. Diffusion changes in the aging human brain. Am. J. Neuroradiol. 21, 1078–1083.
Craik, F.I.M., Morris, L.W., Morris, R.G., Loewen, E.R., 1990. Relations between source amnesia and frontal lobe functioning in older adults. Psychol. Aging 5, 148–151.
Decarli, C., Massaro, J., Harvey, D., Hald, J., Tullberg, M., Au, R., Beiser, A., D'Agostino, R., Wolf, P.A., 2005. Measures of brain morphology and infarction in the Framingham Heart Study: establishing what is normal. Neurobiol. Aging 26, 491–510.
Duncan, J., Owen, A.M., 2000. Common regions of the human frontal lobe recruited by diverse cognitive demands. Trends Neurosci. 23, 475–483.
Fenrich, F.R., Beaulieu, C., Allen, P.S., 2001. Relaxation times and microstructures. NMR Biomed. 14, 133–139.
Filley, C.M., 2001. The Behavioral Neurology of White Matter. Oxford Univ. Press, Oxford.
Folstein, M.F., Folstein, S.E., McHugh, P.R., 1975. Mini-mental state: a practical method for grading the cognitive state of patients for the clinician. J. Psychiatr. Res. 12, 189–198.
Greenwood, P.M., 2000. The frontal aging hypothesis evaluated. J. Int. Neuropsychol. Soc. 6, 705–726.
Hasan, K.M., Parker, D.L., Alexander, A.L., 2001. Comparison of gradient encoding schemes for diffusion-tensor MRI. J. Magn. Reson. Imaging 13, 769–780.
Head, D., Buckner, R.L., Shimony, J.S., Williams, L.E., Akbudak, E., Conturo, T.E., McAvoy, M., Morris, J.C., Snyder, A.Z., 2004. Differential vulnerability of anterior white matter in nondemented aging with minimal acceleration in dementia of the Alzheimer type: evidence from diffusion tensor imaging. Cereb. Cortex 14, 410–423.
Hedden, T., Gabrieli, J.D., 2004. Insights into the ageing mind: a view from cognitive neuroscience. Nat. Rev., Neurosci. 5, 87–96.
Jenkinson, M., 2003. A fast, automated, N-dimensional phase unwrapping algorithm. J. Magn. Reson. Med. 49, 193–197.
Jones, D.K., 2004. The effect of gradient sampling schemes on measures derived from diffusion tensor MRI: a Monte Carlo study. Magn. Reson. Med. 51, 807–815.
Jones, D.K., Williams, S.C., Gasston, D., Horsfield, M.A., Simmons, A., Howard, R., 2002. Isotropic resolution diffusion tensor imaging with whole brain acquisition in a clinically acceptable time. Hum. Brain Mapp. 15, 216–230.
Kemper, T.L., 1994. Neuroanatomical and neuropathological changes during aging and dementia. In: Albert, M.L., Knoefel, J.E. (Eds.), Clinical Neurology of Aging. Oxford Univ. Press, New York, pp. 3–67.
Kubicki, M., Westin, C.-F., Maier, S.E., Mamata, H., Frumin, M., Ersner-Hershfield, H., Kikinis, R., Jolesz, F.A., McCarley, R., Shenton, M.E., 2002. Diffusion tensor imaging and its application to neuropsychiatric disorders. Harvard Rev. Psychiatry 10, 324–336.
Le Bihan, D., 2003. Looking into the functional architecture of the brain with diffusion MRI. Nat. Rev., Neurosci. 4, 469–480.
Marner, L., Nyengaard, J.R., Tang, Y., Pakkenberg, B., 2003. Marked loss of myelinated nerve fibers in the human brain with age. J. Comp. Neurol. 462, 144–152.
Mattis, S., 1988. Dementia Rating Scale (DRS) Professional Manual. Psychological Assessment Resources, Inc., Odessa, FL.
Meier-Ruge, W., Ulrich, J., Bruhlmann, M., Meier, E., 1992. Age-related white matter atrophy in the human brain. Ann. N. Y. Acad. Sci. 673, 260–269.
Mori, S., Kaufmann, W.E., Davatzikos, C., Stieltjes, B., Amodei, L., Fredericksen, K., Pearlson, G.D., Melhem, E.R., Solaiyappan, M., Raymond, G.V., Moser, H.W., van Zijl, P.C., 2002. Imaging cortical association tracts in the human brain using diffusion-tensor-based axonal tracking. Magn. Reson. Med. 47, 215–223.
Moseley, M., 2003. Diffusion tensor imaging and aging—a review. NMR Biomed. 15, 553–560.
Norris, D.G., Niendorf, T., Leibfritz, D., 1994. Healthy and infarcted brain tissues studied at short diffusion times: the origins of apparent restriction and the reduction in apparent diffusion coefficient. NMR Biomed. 7, 304–310.
Nusbaum, A.O., Tang, C.Y., Buchsbaum, M.S., Wei, T.C., Atlas, S.W., 2001. Regional and global changes in cerebral diffusion with normal aging. Am. J. Neuroradiol. 22, 136–142.
O'Sullivan, M., Jones, D., Summers, P., Morris, R., Williams, S., Markus, H., 2001. Evidence for cortical "disconnection" as a mechanism of age-related cognitive decline. Neurology 57, 632–638.
Pfefferbaum, A., Sullivan, E.V., 2002. Microstructural but not macrostructural disruption of white matter in women with chronic alcoholism. NeuroImage 15, 708–718.
Pfefferbaum, A., Sullivan, E.V., 2003. Increased brain white matter diffusivity in normal adult aging: relationship to anisotropy and partial voluming. Magn. Reson. Med. 49, 953–961.
Pfefferbaum, A., Sullivan, E.V., 2005a. Diffusion MR imaging in psychiatry and ageing. In: Gillard, J., Waldman, A., Barker, P. (Eds.), Physiological Magnetic Resonance in Clinical Neuroscience. Cambridge University Press, Cambridge, pp. 558–578 (Chapter 33; invited).
Pfefferbaum, A., Sullivan, E.V., 2005b. Disruption of brain white matter microstructure by excessive intracellular and extracellular fluid in alcoholism: evidence from diffusion tensor imaging. Neuropsychopharmacology 30, 423–432.
Pfefferbaum, A., Sullivan, E.V., Rosenbloom, M.J., Mathalon, D.H., Lim, K.O., 1998. A controlled study of cortical gray matter and ventricular changes in alcoholic men over a five year interval. Arch. Gen. Psychiatry 55, 905–912.
Pfefferbaum, A., Adalsteinsson, E., Spielman, D., Sullivan, E.V., Lim, K.O., 1999a. In vivo brain concentrations of N-acetyl compounds, creatine and choline in Alzheimer's disease. Arch. Gen. Psychiatry 56, 185–192.
Pfefferbaum, A., Adalsteinsson, E., Spielman, D., Sullivan, E.V., Lim, K.O., 1999b. In vivo spectroscopic quantification of the N-acetyl moiety, creatine and choline from large volumes of gray and white matter: effects of normal aging. Magn. Reson. Med. 41, 276–284.
Pfefferbaum, A., Sullivan, E.V., Hedehus, M., Lim, K.O., Adalsteinsson, E., Moseley, M., 2000a. Age-related decline in brain white matter anisotropy measured with spatially corrected echo-planar diffusion tensor imaging. Magn. Reson. Med. 44, 259–268.
Pfefferbaum, A., Sullivan, E.V., Swan, G.E., Carmelli, D., 2000b. Brain structure in men remains highly heritable in the seventh and eighth decades of life. Neurobiol. Aging 21, 63–74.
Pfefferbaum, A., Sullivan, E.V., Carmelli, D., 2001. Genetic regulation of

regional microstructure of the corpus callosum in late life. NeuroReport 12, 1677–1681.
Pfeuffer, J., Van de Moortele, P.F., Ugurbil, K., Hu, X., Glover, G.H., 2002. Correction of physiologically induced global off-resonance effects in dynamic echo-planar and spiral functional imaging. Magn. Reson. Med. 47, 344–353.
Pierpaoli, C., Basser, P.J., 1996. Towards a quantitative assessment of diffusion anisotropy. Magn. Reson. Med. 36, 893–906.
Raz, N., 1999. Aging of the brain and its impact on cognitive performance: integration of structural and functional findings. In: Craik, F.I.M., Salthouse, T.A. (Eds.), Handb. Aging Cogn., vol. II. Erlbaum, Mahwah, NJ, pp. 1–90.
Raz, N., 2004. The aging brain observed in vivo: differential changes and their modifiers. In: Cabeza, R., Nyberg, L., Park, D.C. (Eds.), Cognitive Neuroscience of Aging: Linking Cognitive and Cerebral Aging. Oxford Univ. Press, New York, pp. 17–55.
Raz, N., Gunning, F.M., Head, D., Dupuis, J.H., McQuain, J., Briggs, S.D., Loken, W.J., Thornton, A.E., Acker, J.D., 1997. Selective aging of the human cerebral cortex observed in vivo: differential vulnerability of the prefrontal gray matter. Cereb. Cortex 7, 268–282.
Rumpel, H., Ferrini, B., Martin, E., 1998. Lasting cytotoxic edema as an indicator of irreversible brain damage: a case of neonatal stroke. Am. J. Neuroradiol. 19, 1636–1638.
Sehy, J.V., Ackerman, J.J., Neil, J.J., 2002. Evidence that both fast and slow water ADC components arise from intracellular space. Magn. Reson. Med. 48, 765–770.
Silva, M.D., Omae, T., Helme, r.K.G., Li, F., Fisher, M., Sotak, C.H., 2002. Separating changes in the intra- and extracellular water apparent diffusion coefficient following focal cerebral ischemia in the rat brain. Magn. Reson. Med. 48, 826–837.
Smith, S., 2002. Fast robust automated brain extraction. Hum. Brain Mapp. 17, 143–155.
Sowell, E.R., Thompson, P.M., Holmes, C.J., Jernigan, T.L., Toga, A.W., 1999. In vivo evidence for post-adolescent brain maturation in frontal and striatal regions [letter]. Nat. Neurosci. 2, 859–861.
Sullivan, E.V., Pfefferbaum, A., 2003. Diffusion tensor imaging in normal aging and neuropsychiatric disorders. Eur. J. Radiol. 45, 244–255.
Sullivan, E.V., Adalsteinsson, E., Hedehus, M., Ju, C., Moseley, M., Lim, K.O., Pfefferbaum, A., 2001. Equivalent disruption of regional white matter microstructure in aging healthy men and women. NeuroReport 12, 99–104.
Tisserand, D.J., Jolles, J., 2003. On the involvement of prefrontal networks in cognitive ageing. Cortex 39, 1107–1128.
Virta, A., Barnett, A., Pierpaoli, C., 1999. Visualizing and characterizing white matter fiber structure and architecture in the human pyramidal tract using diffusion tensor MR. Magn. Reson. Imaging 17, 1121–1133.
Woods, R., Grafton, S., Holmes, C., Cherry, S., Mazziotta, J., 1998. Automated image registration: I. General methods and intrasubject, intramodality validation. J. Comput. Assist. Tomogr. 22, 139–152.
Zhang, Y., Brady, M., Smith, S., 2001. Segmentation of brain MR images through a hidden Markov random field model and the expectation maximization algorithm. IEEE Trans. Med. Imaging 20, 45–57.